SUPPORTING INFORMATION

Microfluidic Devices Integrating Microcavity Surface-Plasmon-Resonance Sensors: Glucose Oxidase Binding-Activity Detection

Dragos Amarie[†,*] **Abdelkrim Alileche**[†,**] **Bogdan Dragnea**[‡] **James A. Glazier**[†,*]

Bicomplexity Institute, Department of Physics and Department of Chemistry, Indiana University, Bloomington, Indiana 47405-7102 USA

† Department of Physics & Biocomplexity Institute, Indiana University.
‡ Department of Chemistry & Biocomplexity Institute, Indiana University.
* Corresponding authors e-mail: glazier@indiana.edu, damarie@indiana.edu
** Current address: Department of Biological Sciences, Boise State University, Boise ID.

Table of Contents **1**

Appendix S-1

Time Stability Tests

Our experimental setup (Figure S-1(a)) could collect either spectra (to analyze changes in MSPRS resonances due to refractive-index changes in the fluid or molecular binding to the MSPRS), or time-series (to monitor analyte binding to target-proteins anchored to the MSPRS surface). We investigated molecular interactions by monitoring changes in the emitted-light intensity at a fixed wavelength. We checked the time-stability of our apparatus by filling the chip with a constant-refractive-index fluid flowing at a controlled temperature. Over 12 hours we observed a linear drift of ≈15 counts/s/h, which was less than the ≈50 counts/s noise level.

Appendix S-2

Surface-Plasmon Propagation Wavelength

The SPW wavelength in its direction of propagation is:[1]

(S-1)
$$\lambda_{\mathrm{SP}} = \lambda_0 \sqrt{\frac{\mathrm{Re}(\varepsilon_m) + \varepsilon_2}{\mathrm{Re}(\varepsilon_m)\varepsilon_2}},$$

where $\lambda_0 = 2\pi c / \omega$ is the wavelength of the incident photons in free space, ω is the wave-frequency, c is the speed of light in a vacuum, $\varepsilon_{\mathrm{m}}(\omega) = \mathrm{Re}(\varepsilon_m) + i\,\mathrm{Im}(\varepsilon_m)$ is the complex dielectric function of the metal, $\mathrm{Re}(\varepsilon_m(\omega))$ and $\mathrm{Im}(\varepsilon_m(\omega))$ are the real and imaginary parts of $\varepsilon_{\mathrm{m}}(\omega)$, and ε_2 is the dielectric constant of the sample medium in contact with the MSPRS surface. The surface plasmon’s wavelength is less than the incident photon’s wavelength. For practical materials (silica, glass, quartz), incident light in the UV cannot excite surface-plasmon waves. In the NIR, the surface-plasmon wavelength is proportional to the incident light’s wavelength multiplied by n_2 (Figure S-3).

Appendix S-3

MSPRS vs SPR Sensitivity Estimate

In a very simple model, we consider an ensemble of molecules in solution interacting with target molecules fixed at the sensor's surface. We assume that events occur independently at a certain average rate. The *shot noise* (*Poisson noise*) is defined as:

(S-2) $$N = \sqrt{n},$$

where *n* is the number of molecules interacting with the target molecules.

The recorded signal is:

(S-3) $$S = \alpha n,$$

where α is a sensitivity constant relating the number of molecules involved in the reaction to the real signal recorded from a detector. Combining eqs S-2 and S-3, the signal-to-noise ratio becomes:

(S-4) $$S/N = \alpha\sqrt{n},$$

which gives the sensitivity constant.

Considering the data in Figure 2, the sensitivity ratio is:

(S-5)

$$\frac{\alpha_{MSPRS}}{\alpha_{SPR}} = \frac{\left(S/N\right)_{MSPRS}}{\left(S/N\right)_{SPR}} \frac{\sqrt{n_{SPR}}}{\sqrt{n_{MSPRS}}} = \frac{50.7}{138} \frac{\sqrt{10^{10}}}{\sqrt{1.9 \times 10^{4}}} = 266.$$

Therefore an MSPRS is ≈250 times more sensitive than the Biacore 3000, as determined by the number of molecules required to achieve a given S/N.

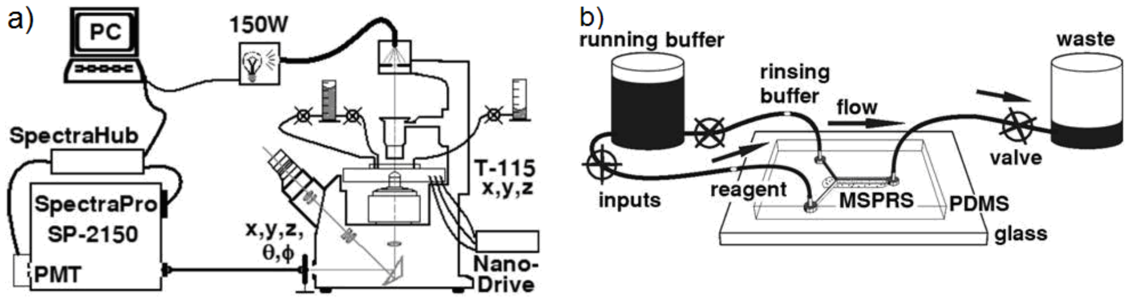

Figure S-1 (a) Schematic of experimental apparatus: the MSPRSs were excited with white light (400–700 nm) and the emitted light analyzed using a software-controlled spectrometer. We selected one MSPRS using a nano-precision stage mounted on a microscope. (b) Schematic of microfluidic chip with fluid control: PDMS-molded microfluidic channels (20 μm deep) are sealed with a cover-glass containing a gold stripe (1 × 10 mm) with ≈500 randomly distributed MSPRSs per mm^2. Two input-channels (50 μm wide, 4 mm long) bring buffer and reagent to the MSPRS chamber. Tubing connecting to the microfluidics is backfilled with 5–10 μL reagent or rinsing buffer. MSPRS chamber flow is controlled hydrostatically. Arrows show flow direction. Not to scale.

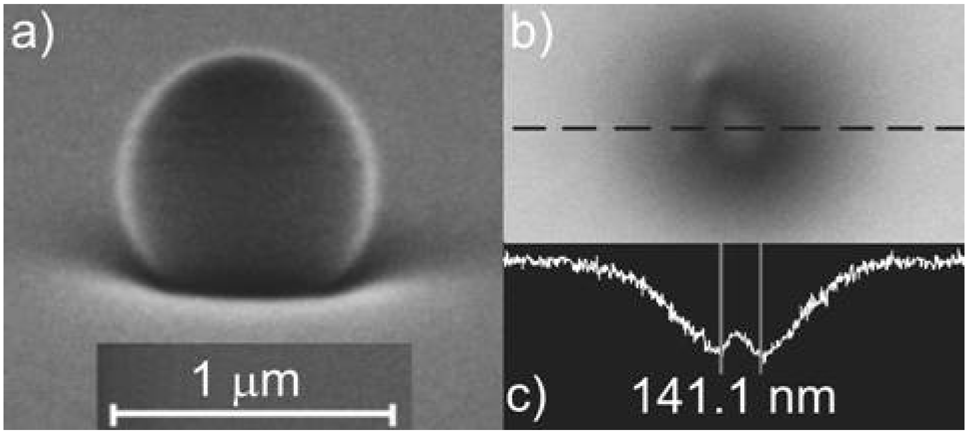

Figure S-2. (a) SEM (75° tilt) of an MSPRS (a 780-nm polystyrene nanosphere placed on a flat glass surface, then uniformly sputtered with a 120 nm gold layer). (b) SEM of a typical sub-wavelength pinhole (viewed from the top) which remains in the gold film after mechanical removal of a MSPRS. The dashed line shows the position of the profile in (c). The bright spot in the middle of the pinhole is a SEM artifact due to charging of the insulating bare glass. Its size reveals the exact shape and size of the pinhole. (c) The nanoaperture profile reveals sharp gold cusps reaching deep under the nanosphere (the vertical axis represents intensity in arbitrary units). Same scale in all panels.

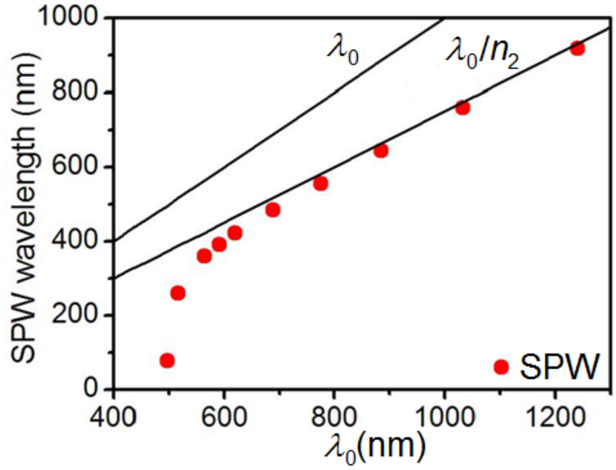

Figure S-3. Surface-plasmon wavelength (using eq S-1) in the direction of propagation at a flat gold-water interface vs incident-photon wavelength (in free space) in the vis-NIR range.[1, 2]

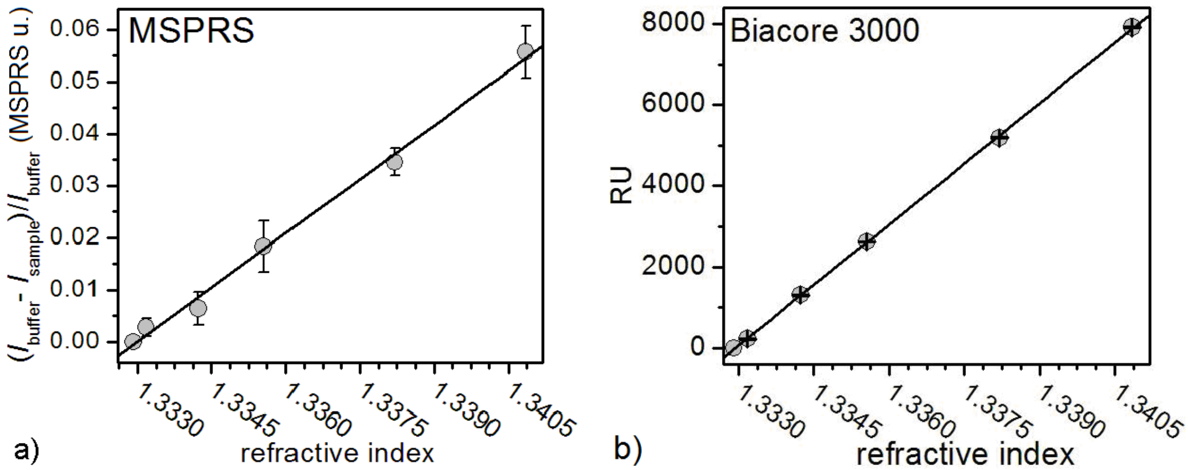

Figure S-4. (a) Normalized MSPRS-emitted intensity change, $(I_{buffer} - I_{solution})/I_{buffer}$, at 640 nm for solutions with various refractive indices: 0%, 0.18%, 0.9%, 1.8%, 3.6% and 5.4% D-Glu in DI-water at 20 °C.[3] We rinsed the bare MSPRS with DI-water for 500 s between 500 s injections. (b) Same experiment on a bare-gold chip, measured using the Biacore 3000. Calibration for bulk fluids only: 10^6 RU = 1 RIU = 6.93 ± 0.24 MSPRS-units.

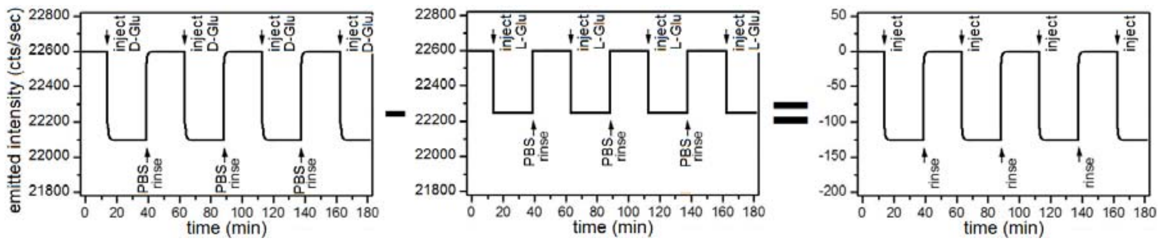

Figure S-5. Schematic of single-MSPRS signal processing to account for the substrate-solution–PBS refractive-index difference during wash-in/wash-out experiments like those in Figures 5a,c and d. We ran four wash-in/wash-out cycles with 100 mM L-Glu and another four wash-in/wash-out cycles with 100 mM D-Glu. We then subtracted the L-Glu signal in each cycle from the corresponding D-Glu signal to obtain the GOx–βD-Glu binding signal.

Supplementary References:

(1) Barnes, W. L. *J. Opt. A: Pure Appl. Opt.* **2006**, *8*, S87-S93.

(2) Weaver, J. H.; Frederikse, H. P. R. In *CRC Handbook of Chemistry and Physics,* 89th ed.; Taylor and Francis Group, LLC., www.hbcpnetbase.com/, **2008-2009**, pp. 124-125.

(3) Lide, D. R., Ed. *CRC Handbook of Chemistry and Physics*, 88th ed.; Taylor and Francis Group, LLC, 2007.